Aalborg Universitet

Power Flow Modeling of Islanded AC Microgrids with Hierarchical Control

Agundis-Tinajero, G.; Segundo-Ramírez, J.; Visairo-Cruz, N.; Savaghebi, M.; Guerrero, J.M.; Barocio, E.

Power Flow Modeling of Islanded AC Microgrids with Hierarchical Control

Gibran Agundis-Tinajero, Juan Segundo-Ramírez, Nancy Visairo-Cruz,

Mehdi Savaghebi, Josep M. Guerrero, Emilio Barocio.

Abstract

This paper presents the power flow modeling of droop-controlled distributed generation units with secondary frequency and voltage restoration control for hierarchically controlled islanded microgrids. These models are incorporated in the conventional Newton-Raphson power flow method as a new bus, without the necessity of a slack bus, and include the gains of the control systems that influence the steady-state solution. Two case studies are addressed. In the first case study, comparisons of the proposed models against the steady-state solutions obtained with PSCAD and Simscape Power System of Simulink, where the closed-loop controls are explicitly modeled, are presented. In the second case study, the proposed method is contrasted against the droop-based approach. The results obtained exhibit low computing effort, reliability, and effectiveness of the proposed models since quadratic convergence behavior is maintained independently of the size and topology of the microgrid. Besides, it is demonstrated that hierarchical and droop controllers lead to different solutions, which confirms the necessity of including the hierarchical control in the power flow model.

Index Terms

Hierarchical control, AC microgrid, Newton-Raphson method, power flow, steady-state solution.

I. INTRODUCTION

MICROGRIDS (MGs) have been introduced as a groundbreaking technology to modernize the electric power systems [1]–[4]. Therefore, important research efforts are currently underway to develop mathematical models and techniques to evaluate and improve their performance, both in the transient and steady state [5], [6]. Regarding the computation of the steady-state solution, this is not a simple task for nonlinear periodic switched networks. One way is to implement the system in professional

G. Agundis-Tinajero, J. Segundo-Ramírez and N. Visairo-Cruz are with the Universidad Autónoma de San Luis Potosí, San Luis Potosí, S.L.P., México (Corresponding author email: gibran.zigma@gmail.com).

J. M. Guerrero and M. Savaghebi are with the Department of Energy Technology, Aalborg University, Aalborg, 9220 Denmark.

E. Barocio is with the Universidad de Guadalajara, Guadalajara, México

time-domain simulation programs, such as PSCAD, Simulink, RSCAD, among others, and simulate until the transient disappears. Even though this is a direct method, it presents some drawbacks, i.e., the controller has to be stable, and the initial condition has to be within the attractor, but the controller tunning and the calculation of proper initial condition are already complicated problems in themselves. Some others techniques based on iterative processes can be used instead of only direct time domain simulation. Some of these techniques are in the time domain [7]–[9], frequency domain [10], [11], extended harmonic domain [12], [13] and hybrid domain [9]. These techniques present better convergence properties such as shorter computation time, the computation of unstable solutions, and those based on the Poincaré map give as byproduct the Floquet multipliers of the computed solution; however, these methods also have drawbacks, such as, the computational burden, the sensitivity of the correct computation of the transition matrix, among others, for more details see these references [14], [15]. In power systems industry, the common way to compute the steady-state is solving the power balance equation using the Newton method [16]. As compared with synchronous generators in conventional power systems, the injected active and reactive power by the distributed generation (DG) units in microgrids are not usually known at the starting of the Newton iterations since they depend on their specific control systems [17]–[19]. Additionally, in the islanded operation mode, the frequency of the system can be different from the nominal and the so-called slack bus is missing [20], [21]. Despite that the slack bus could be reassigned or distributed in an islanded situation, the DG unit selected as slack bus should be able to provide all the missing active and reactive power, but it could not always be possible due to their limited and not dispatchable capacity [2], [22].

Microgrids control requirements and strategies to perform local balancing and to maximize their benefits have led the MGs to fulfill a wide range of functionalities, such as power flow control to avoid exceeding line capacities, voltage and frequency regulation, energy balance, among others [18], [23]–[25]. In this way, practical MGs include hierarchical control schemes to achieve the desired operational requirements. Consequently, since the hierarchical controls modify the steady-state operation of the MG, they have to be included in the methods for the computation of the steady-state. Hierarchical control systems increase the difficulty of the power flow modeling since their secondary and tertiary controls change the operating points of the MGs, such that, the active and reactive power injected by the DG units differ from those injected by DG units with only droop control. Keep in mind that the tertiary control level typically operates in the order of minutes [17]. Therefore, their outputs can be considered constant in the power flow modeling; however, the operation time of the secondary control, such as the frequency and voltage restoration control, is close to the primary control operation time. Hence, the outputs of the secondary control cannot be assumed as constant inputs to the primary control. For these reasons, the power flow model must include primary and secondary controllers.

In the literature, it can be found that several authors have addressed the power flow problem for islanded droop-controlled microgrids [2], [20], [22], [26]–[33]. For example, a three phase generalized power flow for islanded microgrids using a Newton trust region method is presented in [22], it takes into account the droop characteristics of the DG units and unbalances in the microgrid, furthermore, a comparison with PSCAD is performed using a six-bus MG, achieving maximum errors of 0.5% and 0.05% in phase and voltage magnitude, respectively. In [20], an interior point-based power flow for balanced droop based microgrids is developed. The method is compared against PSCAD using a six-bus MG, the maximum absolute error achieved is $1.689{\times}10^{-2}$; besides, the computing time needed by the method was 0.23748 seconds. Virtual impedances have been included in the power flow computation in [2]. A particle swarm optimization to solve the power flow problem in islanded microgrids is performed in [26], where the stability of the system is also ensured. In [27], the authors proposed the inclusion of the droop equations in the conventional power flow formulation, with the purpose of having a straightforward method that can be integrated into current commercially available power system software. Comparisons against PSCAD were presented in the paper, being the maximum voltage magnitude and phase angle error achieved of $2{\times}10^{-4}$ and $8.5{\times}10^{-3}$, respectively. An AC/DC load flow algorithm for islanded microgrids taking into account the droop characteristics is presented in [28], the load flow is solved sequentially, having as subsystems the AC system and the DC system, using a modified directed forward-backward sweep method. In [29], a branch-based power flow for islanded microgrids is shown, a forward-return-forward-sweep method including droop controls is proposed in this work. In [30] a review of power flow methods for droop-based islanded microgrids is addressed, the authors compare the algorithms in terms of accuracy and convergence time, besides, a method based on particle swarm optimization is presented. Reference [32] presents a methodology to extend the conventional power flow method to islanded microgrids; however, only considers droop controls. Furthermore, the authors present a seven-bus case and the method converges in 2.065 seconds. A generic modeling approach for droop-controlled and isochronous MGs is presented in [31]; the authors develop models for different primary control operation schemes and unbalanced conditions; however, only includes primary controls. Recently, reference [33] presents a generalized microgrid power flow method for radial and weakly meshed topologies, which includes primary and secondary control schemes. The authors use a direct backward/forward sweep method, where the power flow problem is solved sequentially in a double-loop process deteriorating the convergence rate; a case study is presented, but no comparison results against other methods are performed, and only uses linear loads. Additionally, the authors state that the algorithm convergence depends on the stability of the microgrid controllers.

This paper presents the power flow modeling of the hierarchically controlled DG units with primary

droop-based and secondary frequency and voltage restoration controls to cope with the problems mentioned above. The obtained models are represented as a new bus type embedded in the conventional Newton-Raphson power flow [16]. Therefore, the method maintains its quadratic convergence regardless of the microgrid topology, stability, control tunning, and its nonlinear loads. Furthermore, the method preserves explicitly the control gains that influence the steady-state solution.

One of the main issues of islanded microgrids, in the context of the power flow formulation, is that the slack bus does not exist [2]. In this regard, it is demonstrated that the frequency restoration term is related to the bus phase angle where the secondary control regulates the voltage. Consequently, this phase angle becomes the reference angle for the DG units, thus, the slack bus is not needed, but all the units (grid-forming units) participate in sharing the injected power according to the hierarchical control. This feature is a fundamental advantage because it avoids the use of an adaptive slack bus [33] or the fixing of a bus phase angle to zero [2]. The steady-state solutions obtained with the proposed Newton-Raphson based power flow are compared against the steady-state solutions obtained with time-domain implementations in industrial electromagnetic transient simulation programs.

The paper is organized as follows: Section II describes the hierarchical control considered for the proposed power flow formulation. Section III introduces the formulation of the proposed power flow model which includes the primary droop control and the secondary frequency and voltage restoration control. Section IV describes the microgrid used as the test system. Section V outlines the case studies and presents results obtained. Finally, Section VI provides the conclusions of this work.

II. HIERARCHICAL CONTROL

In order to operate the microgrid in a controlled manner, a two-level hierarchical control scheme is included [18]. The scheme is composed by a local primary control, a secondary control for frequency and voltage restoration, and a synchronous reference frame phase-locked loop (SRF-PLL) [34] for measuring the voltage magnitude ($|V_m|$) and frequency (ω_m) of the m-th bus of the system, as seen in Fig. 1.

The primary control level, which is modeled in the dq-reference frame, is responsible for performing the grid-forming function, and its structure is shown in Fig. 2. This level consists of a conventional droop control, in which, the active and reactive power contribution of the n-th DG unit depends on the frequency/active power (P-ω) and voltage/reactive power (Q-V) droop characteristic curves, respectively, being expressed as [35],

$$\omega_n = \omega^* - K_n^p P_n \tag{1}$$

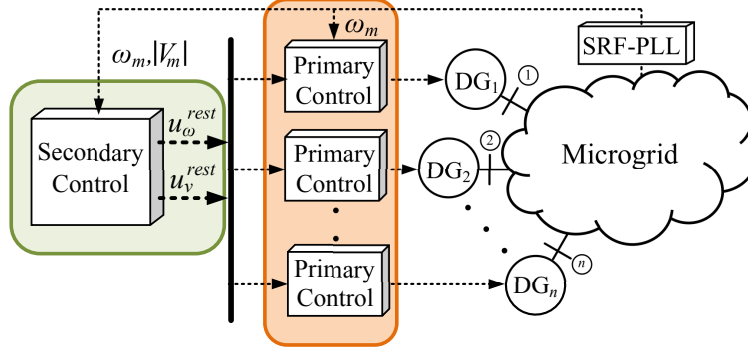$$|V_n| = |V_n^*| - K_n^q Q_n \tag{2}$$

Fig. 1. Hierarchical control scheme.

where ω^* is the nominal angular frequency of the system, $|V_n^*|$ is the voltage amplitude reference, and K_n^p and K_n^q are the P-ω and Q-V droop coefficients, respectively [35]. Additionally, this stage includes an inner current control loop and an outer voltage control loop which define the control signals for operating each DG unit with a given amplitude V_n and frequency ω_n, as shown in Fig. 2 [19].
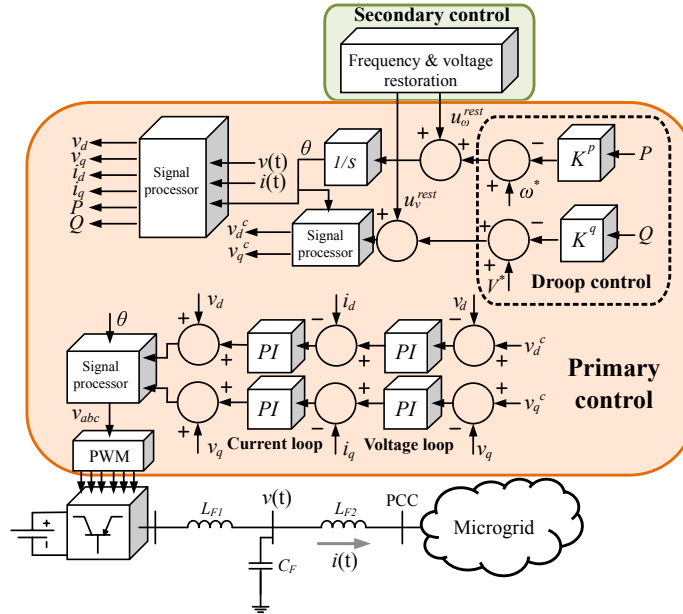
Fig. 2. Hierarchical control block diagram.

On the other hand, the secondary control level is responsible to compensate the MG frequency and voltage deviations [18]. This control measures the system frequency and bus voltage and compares them against the references ω^* and $|V_m^{**}|$, respectively. Note that, $|V_n^*|$ is the voltage reference for the primary control, and $|V_m^{**}|$ is the voltage reference for the secondary control. The error in each case of the secondary control is processed through a proportional-integral (PI) controller to obtain the output signals u_ω^{rest} and u_v^{rest}, as follows,

$$u_\omega^{rest} = k^{pw}(\omega^* - \omega_m) + k^{iw} \int (\omega^* - \omega_m)dt \qquad (3)$$

$$u_v^{rest} = k^{pv}(|V_m^{**}| - |V_m|) + k^{iv} \int (|V_m^{**}| - |V_m|)dt \qquad (4)$$

where ω_m and $|V_m|$ are the angular frequency and the voltage magnitude measured in the m-th bus, respectively. In this bus, the secondary control restores the frequency and voltage magnitude. It is important to mention that the secondary frequency control works using the SRF-PLL measurements, and these influence the DG units output phase.

The output signals u_ω^{rest} and u_v^{rest} are sent to each DG unit to restore the frequency and voltage deviations after every change in the microgrid, therefore, the equations (1) and (2) are modified as follows,

$$\omega_n = \omega^* - K_n^p P_n + u_\omega^{rest} \qquad (5)$$

$$|V_n| = |V_n^*| - K_n^q Q_n + u_v^{rest} \qquad (6)$$

Observe that in a microgrid with a point of common coupling (PCC), both frequency and voltage restoration controllers are controlling the same bus; however, in the case of a multi-bus microgrid, the voltage restoration control can be distributed in the different buses of the DG units [36].

As mentioned in the Introduction, due to the tertiary control level typically operates in the order of minutes, their outputs can be considered constant for the power flow modeling, therefore, the tertiary control is not included in the hierarchical control shown in this section; however, the function of this level concerns with the optimal operation of the microgrid subject to different objectives such as economical dispatch, power flow balance, stability, among others [18], [25], [36], [37]. In this way, the tertiary control, based on nominal reference values, modifies the primary and secondary control references (V^{**}, K^p, K^q) depending on the operational objectives selected. For example, the modification of K^p and K^q, changes the active and reactive power dispatch ratio among the DG units [18]. On the other hand, the reference voltage V^{**}, which is used to restore the voltage deviations can be modified when the secondary voltage control is distributed to control the DG units reactive power injection [36]; in the case of a single PCC, the secondary voltage control is used to restore the voltage deviation due to the primary control.

III. POWER FLOW MODELING

In the conventional power flow method [16], all buses fall within only three types: voltage controlled bus (PV), load bus (PQ), and slack bus. Using these bus models, the DG units operating in PV and PQ

mode can be represented in the power flow problem [38]. However, the droop-controlled DG units cannot be modeled by any of the typical buses (PV, PQ, and slack). To cope with this problem, a new bus, called droop bus, was introduced [22]. Nevertheless, none of these bus types can represent the droop-controlled DG units with secondary control for frequency and voltage restoration. In this regard, this section presents the procedure for the incorporation of the hierarchically controlled DG units for islanded AC microgrids in the well-known power flow method [16].

A. Active power droop control and frequency restoration formulation

The active power output of each DG unit is governed by equation (5), which in turn depends on the frequency restoration output of the secondary control. According to (5), with $\omega_m = \omega^*$ and where the subscript m indicates the bus controlled by the secondary control, the active power reference of the n-th DG unit becomes,

$$P_n^{ref} = \frac{u_\omega^{int}}{K_n^p} \tag{7}$$

where u_ω^{int} is the output of the frequency secondary control integrator $\left(k^{iw} \int (\omega^* - \omega_m)dt\right)$ in steady-state and it is calculated as follows.

The bus phase angle θ_m, where the secondary control measures the frequency, is related with the angle δ_m in the following way,

$$\theta_m = \omega^* t + \delta_m \tag{8}$$

where t is the time. Observe that if (8) is derived with respect to the time, the following expression results,

$$\frac{d\delta_m}{dt} = \omega_m - \omega^* \tag{9}$$

Thus, (9) can be substituted in the integral part of (3); then by integrating u_ω^{int}, the following expression is obtained,

$$u_\omega^{int} = -k^{iw}(\delta_m - \delta_m^0) \tag{10}$$

where δ_m^0 is an initial condition. Note that, if the phase reference is shifted due to the SRF-PLL measurements as mentioned in Section II, the change is reflected in δ_m^0. In this work the SRF-PLL measures the q voltage component (v_q), therefore, the output will be shifted 90 degrees.

Merging (7) and (10), it is observed that P_n^{ref} depends on the bus angle (δ_m) where the bus is being controlled by the secondary control, the integration gain (k^{iw}), the droop gain (K_n^P), and the initial constant value,

$$P_n^{ref} = \frac{-k^{iw}(\delta_m - \delta_m^0)}{K_n^P} \tag{11}$$

Therefore, using (11) and scaling it to p.u., the equation that has to be solved for the active power ΔP_n is as follows,

$$\Delta P_n = P_n - P_n^{ref} = P_n - \frac{-k^{iw}(\delta_m - \delta_m^0)}{K_n^P} \frac{1}{S_{base}} \tag{12}$$

Note that in eq. (12) only appears the control gains that modify the steady-state solution. Furthermore, it is shown that the secondary control sets the reference phase angle for all the DG units. This finding shows that, regarding power flow formulation, the slack bus is not needed, but instead, all the DG units share the injected power. Consequently, the use of an adaptive slack bus [33] or the fixing of a bus phase angle to zero [2] are avoided.

B. Reactive power droop control and voltage amplitude restoration formulation

According to (6), the power flow model for the reactive power of the n-th DG unit, can be written as follows,

$$Q_n^{ref} = \frac{|V_n^*| - |V_n| + u_v^{int}}{K_n^q} \tag{13}$$

where u_v^{int} is the integrator output of the secondary voltage control in steady-state. In this case, there is no equation related to the integral part of the secondary voltage control such as in the secondary frequency part; however, it is known that in steady-state, the voltage at the controlled bus is going to be fixed to the value of the secondary voltage control reference ($|V_m| = |V^{**}|$), therefore, the reactive power equation related to the controlled bus is used to compute the value of u_v^{int}. In this way, there is no change in the formulation due to the secondary voltage control and the reactive power formulation ΔQ_n is as follows,

$$\Delta Q_n = Q_n - \frac{|V_n^*| - |V_n| + u_v^{int}}{K_n^q} \frac{V_{base}}{S_{base}} \tag{14}$$

Finally, the mismatching equations of the new controlled bus needed by the power flow formulation, which will be called as hierarchically controlled PQ (HCPQ) bus from now on, can be summarized as follows,

$$\begin{bmatrix} \Delta P_n \\ \Delta Q_n \end{bmatrix} = \begin{bmatrix} P_n - \dfrac{-k^{iw}(\delta_m - \delta_m^0)}{K_n^P} \dfrac{1}{S_{base}} \\ Q_n - \dfrac{|V_n^*| - |V_n| + u_v^{int}}{K_n^q} \dfrac{V_{base}}{S_{base}} \end{bmatrix} \qquad (15)$$

Now, each hierarchically controlled DG unit can be included in the power flow model in the form of the new HCPQ bus, shown schematically in Fig. 3.
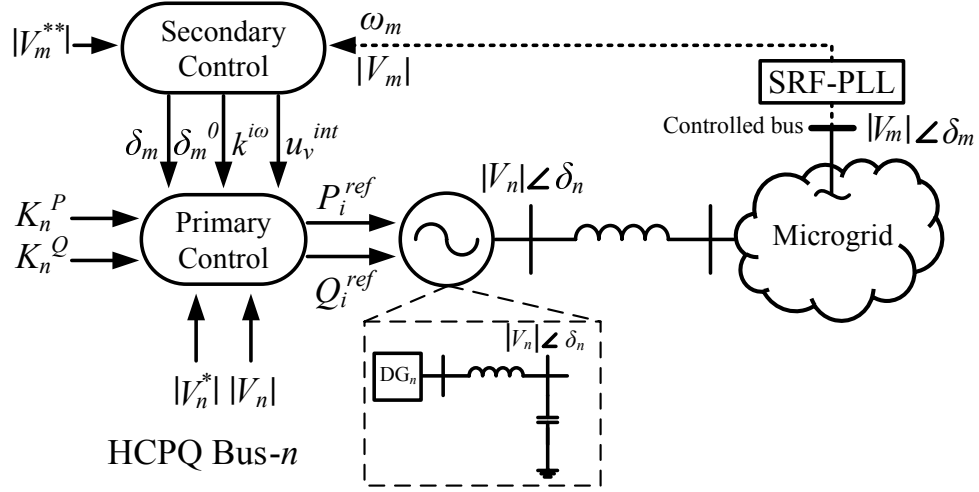

Fig. 3. HCPQ bus diagram.

According to (13), the controlled reactive power is based on the measured capacitor voltage shown in Fig. 3, and this voltage is adjusted by the primary control; thus the LC filter is embedded in the HCPQ bus.

C. Reactive power droop control and voltage amplitude restoration: system reduction

Observe that, if the DG units are connected to the bus where the voltage is restored by the secondary control, a reduction of the system can be made. For explanation, Fig. 4 shows the single-line diagram of a DG unit connected through a feeder to the PCC where the secondary control restores the voltage.
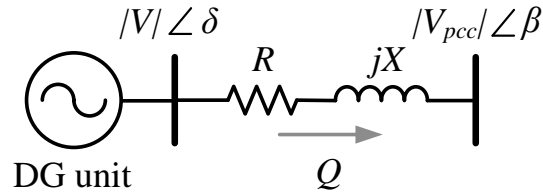

Fig. 4. Single-line diagram of a DG unit connected to the PCC bus.

From Fig. 4, the reactive power flowing from the DG unit to the PCC, can be computed as,

$$Q = - \left(|V|^2 |Y| sin(\theta) - |V||V_{pcc}||Y| sin(-\delta + \beta + \gamma) \right) \tag{16}$$

where $|V_{pcc}|$ is known since it is a controlled voltage ($|V_{pcc}| = |V^{**}|$), β is the phase angle of $|V_{pcc}|$, as seen in Fig. 4, and γ is the admittance angle. Merging Eqs. (13) and (16) yields to,

$$|V|^2 |Y| sin(\gamma) - |V||V_{pcc}||Y| sin(-\delta + \beta + \gamma)$$
$$+ \frac{|V^*| - |V| + u_v^{int}}{K^q} \frac{V_{base}}{S_{base}} = 0 \tag{17}$$

this equation can be rearranged as,

$$|V|^2 |Y| sin(\gamma) + |V|(-|V_{pcc}||Y| sin(-\delta + \beta + \gamma)$$
$$- \frac{1}{K^q} \frac{V_{base}}{S_{base}}) + \frac{|V^*| + u_v^{int}}{K^q} \frac{V_{base}}{S_{base}} = 0 \tag{18}$$

Computing the roots of (18), the voltage $|V|$ can be obtained. In this way, since the voltage of the new controlled bus HCPQ is already known, the mismatching equations needed in the power flow formulation are reduced as follows,

$$\Delta P_n = P_n - \frac{-k^{iw}(\delta_m - \delta_m^0)}{K_n^P} \frac{1}{S_{base}} \tag{19}$$

Finally, combining the model of HCPQ from equation (15), and the PV and PQ buses from the conventional power flow method, the power flow formulation of the whole system can be summarized as follows,

$$\left. \begin{array}{l} P_n - \dfrac{-k^{iw}(\delta_m - \delta_m^0)}{K_n^P} \dfrac{1}{S_{base}} = 0 \\ Q_n - \dfrac{|V_n^*| - |V_n| + u_v^{aux}}{K_n^q} \dfrac{V_{base}}{S_{base}} = 0 \end{array} \right\} \text{HCPQ bus}$$

$$\left. \begin{array}{l} P_n - P_n^{sch} = 0 \\ Q_n - Q_n^{sch} = 0 \end{array} \right\} \text{PQ bus} \tag{20}$$

$$P_n - P_n^{sch} = 0 \left. \right\} \text{PV bus}$$

where P_n and Q_n are the injected active and reactive powers [39], respectively, and they are expressed as,

$$P_n = \sum_{m=1}^{M} |V_n||V_m||Y_{nm}|cos(\gamma_{nm} - \delta_n + \delta_m)$$

$$for \ n = 1, ..., N \tag{21}$$

$$Q_n = -\sum_{m=1}^{M} |V_n||V_m||Y_{nm}|sin(\gamma_{nm} - \delta_n + \delta_m)$$

$$for \ n = 1, ..., N \tag{22}$$

Note that The HCPQ bus can be replaced by equation (19) if the DG units are connected to the bus controlled by the secondary voltage control. In order to have a better understating of the power flow method, a flowchart is presented in Fig. 5.
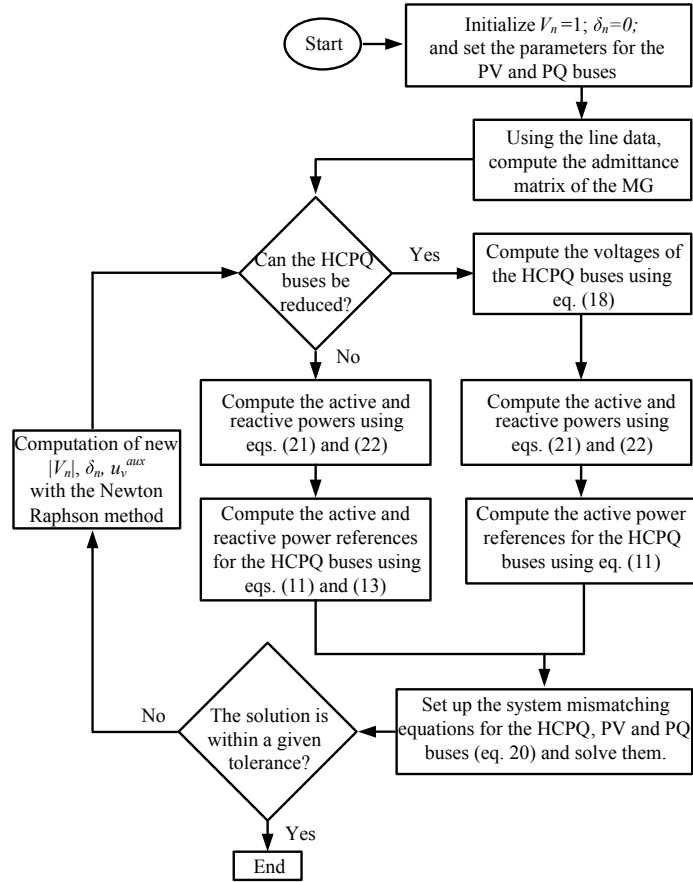

Fig. 5. Power flow method flowchart.

IV. CASE STUDY SYSTEM

Figure 6 shows the single-line diagram of the test system. The microgrid includes 5 DG units and an AC voltage source. The DG units and AC voltage source interact with each other through RL lines and

TABLE I

PARAMETERS OF THE CASE STUDY MICROGRID AND CONTROL

| Parameter	Symbol	Value
Nominal voltage	V_{L-L}^{RMS}	400 V
Nominal frequency	f^*	50 Hz
Nominal DC voltage	V_{DC}	1500 V
Filter resistance	$R_{11}, R_{12}, R_{21},$ R_{22}, R_{31}, R_{32}	0.1 Ω
Filter inductance	$L_{11}, L_{21}, L_{31},$	1.8 mH
Filter capacitance	C_{11}, C_{21}, C_{31}	27 μF
Feeder resistance	R_{13}, R_{23}, R_{33}	0.1 Ω
Feeder inductance	L_{12}, L_{22}, L_{32}	1.25 mH
Current loop proportional gain	k_{pc}	20
Current loop integral gain	k_{ic}	40
Voltage loop proportional gain	k_{pvo}	2.4×10^{-2}
Voltage loop integral gain	k_{ivo}	4.5
Frec. rest. proportional gain	k^{pw}	0.02
Frec. rest. integral gain	k^{iw}	4
Voltage rest. proportional gain	k^{pv}	0.2
Voltage rest. integral gain	k^{iv}	4
Switching frequency	f_c	10 kHz
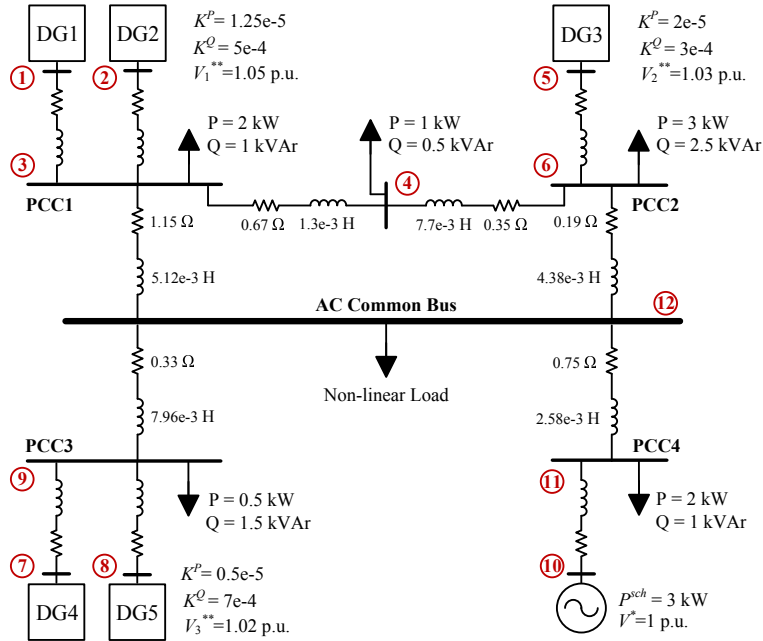
Fig. 6. Single-line diagram of the second case study microgrid.

share the AC common bus where the secondary frequency control acts; the secondary voltage control acts at the different PCCs [36]. The microgrid contains linear loads and a voltage-dependent non-linear load connected to the AC common bus. The HCPQ buses represent the DG units, the PQ buses represent the loads, and the PV bus represent the AC voltage source. Table I shows the parameters of LC filters, feeders, and primary controls. The case study considers the same PI control gains for all the DG units; however, the droop characteristics are different for the DG units as shown in Fig. 6. Additionally, the line impedances and the voltage references for the restoration control ($|V^{**}|$), are also shown in Fig. 6; the parameters of the line impedances were extracted from [40]. The proportional and integral gains were calculated based on stability constrains. This was performed based on a small-signal analysis previously proposed, interested readers may refer to [41] in which a small-signal stability analysis is performed for an islanded microgrid.

The nonlinear industrial load at bus 12 expressed as [20],

$$P_{L,12} = P_{L,12}^0 V_{12}^{\alpha} \tag{23}$$

$$Q_{L,12} = Q_{L,12}^0 V_{12}^{\beta} \tag{24}$$

where $\alpha = 0.18$, $\beta = 6$, $P_{L,12}^0 = 0.5$ p.u., $Q_{L,12}^0 = 0.3$ p.u., and $S_{base} = 10$ kVA.

V. POWER FLOW MODEL EVALUATION

This section presents two evaluation cases of the proposed power flow model for hierarchically controlled islanded microgrids. In the first case, a comparison among the obtained steady-state solutions with the proposed models, and the steady-state solutions obtained with the complete time-domain models using two professional simulators, PSCAD and MATLAB/Simulink, is performed. Additionally, presents an analysis of the convergence behavior for different X/R transmission line ratios in resistive microgrids.

In order to show the difference in the solutions obtained between a hierarchically-controlled MG and a droop-controlled MG, the second case study presents the differences between the power flow solutions obtained with the hierarchical control (HCPQ bus), and with the primary control (droop bus) against the variation of the load 4. The load 4 is varied as follows,

$$P_{L,4} = P_{L,4}^0 (1 + \lambda) \tag{25}$$

$$Q_{L,4} = \sqrt{\frac{P_{L,4}^2}{PF_{L,4}^2} - P_{L,4}^2} \tag{26}$$

where λ is the loading factor, and *PF* is the power factor of the load. Additionally, in this case the secondary voltage control reference is $|V^{**}| = 1$ for all the DG units, and the nominal bus 4 load is $P_{L,4}^0 = 15$ kW with a lagging power factor of 0.89.

The power flow equations are solved using the Newton-Raphson method. The MATLAB/Simulink simulations are conducted using the fundamental frequency model, using the *ode15s* integration method with absolute and relative tolerances of 1×10^{-6}. On the other hand, PSCAD enables the switching process of the power electronic interface of the DG units, using an integration time step of 0.05×10^{-6}. The studies were performed in a MacBook Pro with a processor of 2.5 GHz Intel Core i5 and 16 GB of RAM. A convergence error tolerance of 1×10^{-8} was used.

A. Case Study I: meshed multi-bus microgrid

Table II shows steady-state voltage magnitudes and phase angles given by the power flow solution, MATLAB/Simulink, and PSCAD. Observe that in the worst case, the proposed power flow gives errors of 5.112×10^{-6} and 1.581×10^{-3} as compared to MATLAB/Simulink and PSCAD, respectively. The errors are due to the different modeling approaches, the time steps, and the integration methods. In the case of PSCAD, the additional active and reactive power losses owing to the harmonic distortion generated by the power electronics inverters of each VSC increase the differences.

Figure 7 shows the active and reactive powers injected by the DG units, computed with the power flow method, MATLAB/Simulink, and PSCAD. The obtained results corroborate the effectiveness of the proposed power flow modeling to represent the hierarchical control of the MG.

TABLE II

CASE STUDY I: COMPUTED VOLTAGES WITH THE PROPOSED POWER FLOW METHOD, SIMULINK AND PSCAD

| Bus	Power Flow (PF)	Simulink (averaged model)	PSCAD (switched model)	Error of PF vs. Simulink	Error of PF vs. PSCAD
1	$1.0585268\ \underline{/88.176199^o}$	$1.0585276\ \underline{/88.176313^o}$	$1.0569459\ \underline{/88.173563^o}$	2.252×10^{-6}	1.581×10^{-3}
2	$1.0585268\ \underline{/88.176199^o}$	$1.0585276\ \underline{/88.176313^o}$	$1.0569459\ \underline{/88.173563^o}$	2.252×10^{-6}	1.581×10^{-3}
3	$1.05\ \underline{/88.103490^o}$	$1.0499999\ \underline{/88.103605^o}$	$1.0484303\ \underline{/88.099824^o}$	2.109×10^{-6}	1.571×10^{-3}
4	$1.0430266\ \underline{/88.297780^o}$	$1.0430265\ \underline{/88.297838^o}$	$1.0414725\ \underline{/88.295259^o}$	1.060×10^{-6}	1.554×10^{-3}
5	$1.0405431\ \underline{/88.483247^o}$	$1.0405448\ \underline{/88.483304^o}$	$1.0390094\ \underline{/88.486513^o}$	1.990×10^{-6}	1.534×10^{-3}
6	$1.03\ \underline{/88.508686^o}$	$1.0300001\ \underline{/88.508744^o}$	$1.0284684\ \underline{/88.510806^o}$	1.047×10^{-6}	1.532×10^{-3}
7	$1.0240570\ \underline{/95.913364^o}$	$1.0240571\ \underline{/95.913650^o}$	$1.0224847\ \underline{/95.918692^o}$	5.112×10^{-6}	1.575×10^{-3}
8	$1.0240570\ \underline{/95.913364^o}$	$1.0240571\ \underline{/95.913650^o}$	$1.0224847\ \underline{/95.918692^o}$	5.112×10^{-6}	1.575×10^{-3}
9	$1.02\ \underline{/95.463305^o}$	$1.0199999\ \underline{/95.463592^o}$	$1.0184334\ \underline{/95.467373^o}$	5.110×10^{-6}	1.568×10^{-3}
10	$1\ \underline{/91.212589^o}$	$0.9999999\ \underline{/91.212646^o}$	$0.9984393\ \underline{/91.212646^o}$	9.998×10^{-7}	1.560×10^{-3}
11	$1.0021472\ \underline{/90.733596^o}$	$1.0021462\ \underline{/90.733539^o}$	$1.0005936\ \underline{/90.733768^o}$	1.412×10^{-6}	1.553×10^{-3}
12	$1.0110652\ \underline{/89.745931^o}$	$1.0110633\ \underline{/89.745989^o}$	$1.0095279\ \underline{/89.746447^o}$	2.158×10^{-6}	1.537×10^{-3}
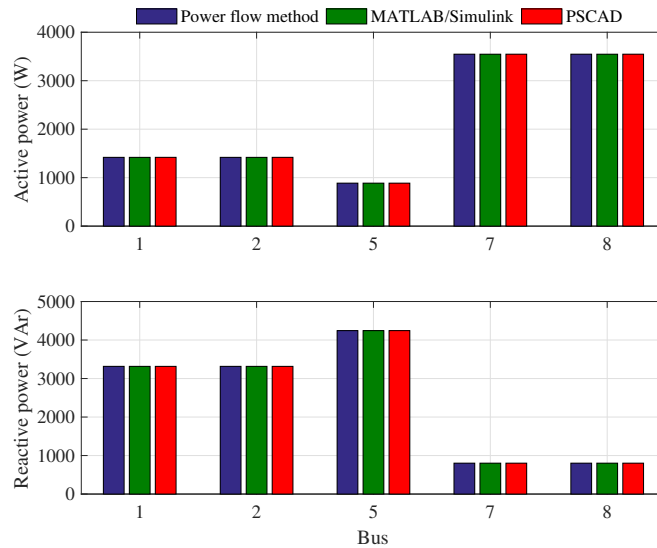
Fig. 7. Comparison of the active and reactive powers injected by the DG units given by the power flow method, MATLAB/Simulink and PSCAD in Case I.

Some essential features of the power flow are the computational speed and convergence rate, in this regard, Table III shows its convergence mismatches and CPU time. Notice that the method has a quadratic convergence characteristic and achieve a convergence error of 8.519×10^{-11} in only four iterations at 0.145 seconds.

As is shown in this case study, the power flow method has a good performance regarding the execution

Iteration	Power Flow
1	1.644×10^{-2}
2	1.449×10^{-3}
3	4.813×10^{-6}
4	8.519×10^{-11}
CPU time	0.145 s

time and convergence rate. Furthermore, the steady-state solution obtained with the proposed power flow model is as good as the one obtained with the professional time-domain simulation programs. To evaluate the convergence characteristic of the proposed power flow in a dominantly resistive MG, the transmission lines parameters of the microgrid of Fig. 6 were changed to reduce their X/R ratio 16 times. Line inductances were reduced four times, and line resistances were increased four times. Under this condition, the Newton-Raphson method converges in 6 iterations with an error of 2.2297×10^{-13}, but still preserves its quadratic convergence feature.

B. Case Study II: Power flow comparison, HCPQ bus against droop bus

Figure 8 shows the differences between the bus voltages obtained with the proposed HCPQ bus and the droop bus, versus load changes. Notice that the voltage magnitude differences ($V_{Hierar} - V_{Droop}$) are positive since the voltage drop with the droop-based control is larger in all buses, except bus 10 because it is a PV bus. This behavior is expected since the droop-based control does not restore the voltage deviations. Furthermore, the voltage drops with the droop-based control increase the currents, which provoke an increment of losses as compared with the hierarchical control.

On the other hand, the phase angles differences show positive and negative evolutions, which also increase as the load increases. As mentioned before, the reference angle is imposed by the secondary control, therefore, as shown in Fig. 8, the phase angles achieved by the hierarchically controlled MG case are different to those obtained with the droop-based controlled MG case, in which case, a phase angle has to be fixed.

Figure 9 shows the differences between the powers injected by the hierarchically controlled MG and the droop-based controlled MG under variation of the load at bus 4. Observe that for light loads, the injected active powers by both control schemes are close each other; however, for larger loads, the differences increases, except for bus 10 because it is a PV bus. Note that the differences increase considerably for large loads, being the droop-based approach the one that has more significant active power injections. Please notice that in the droop control case, the DG units inject more reactive power than in the hierarchically
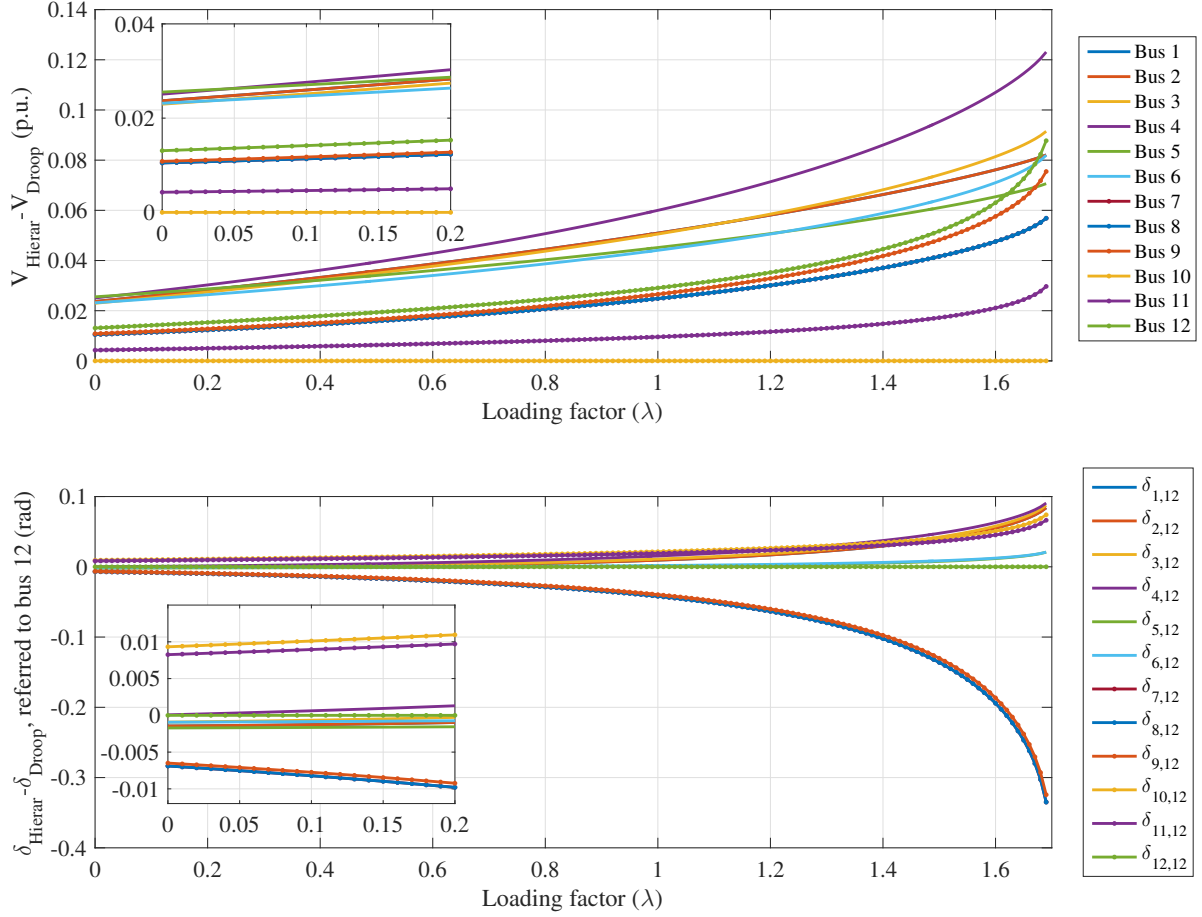
Fig. 8. Differences of the steady-state buses voltage magnitudes and phase angles, solving the system with the power flow method using the HCPQ bus and the droop bus, for the bus 4 load variation.

controlled case. This behavior is owing to the lack of voltage regulation, which also causes more power losses.

The differences shown in this case study, exhibit the importance of using hierarchically controlled power flow models when the DG units include secondary controls for voltage and frequency restoration. Power flow based analyses are widely used in industry. Therefore, accurate modeling is essential to achieve reliable steady-state solutions. It is demonstrated that the proposed HCPQ bus enhances the reliability of power flow solution of hierarchically controlled islanded microgrids.

VI. CONCLUSION

This paper has introduced a methodology to include the hierarchical control of islanded microgrids with a primary droop-based control and a secondary control for frequency and voltage restoration in the well-known power flow method. The proposed power flow models have been validated against the steady-state
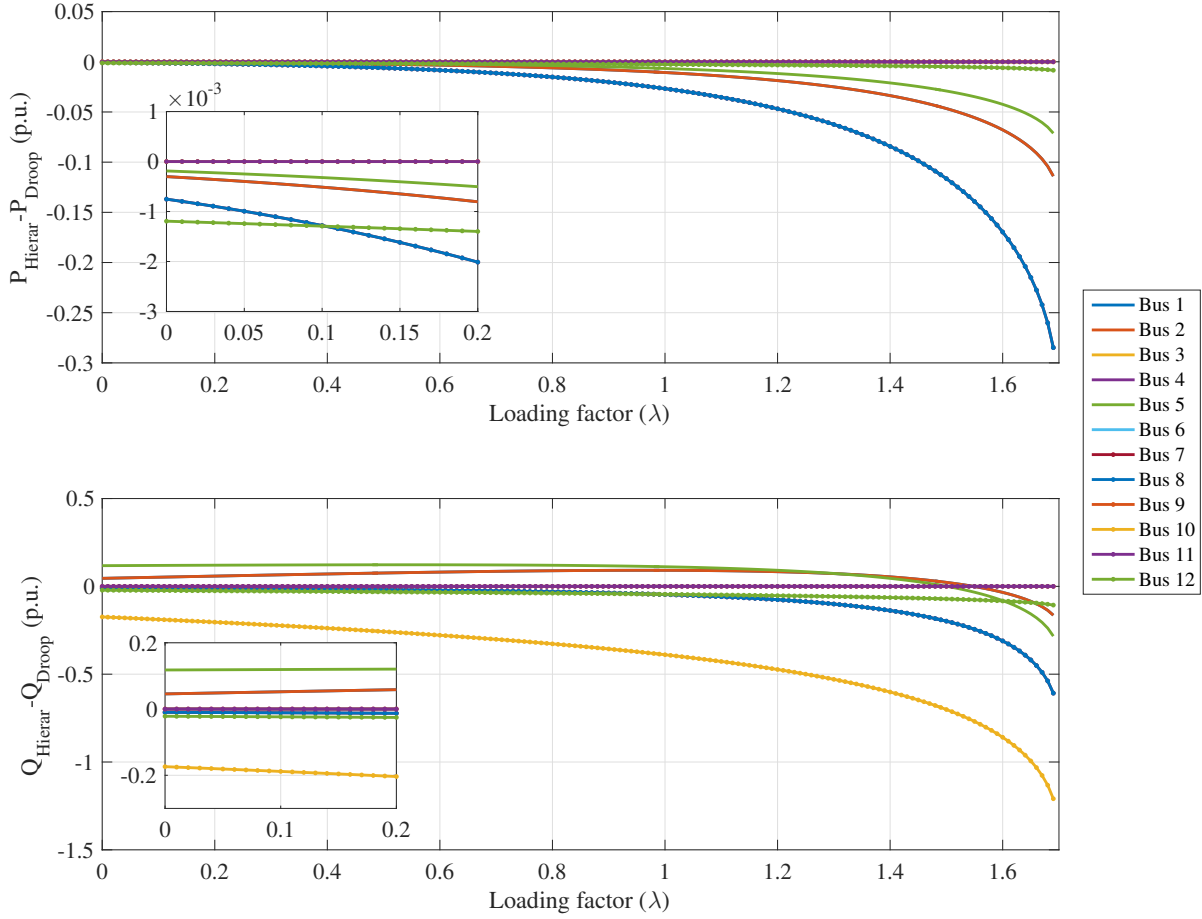
Fig. 9. Differences of the steady-state active and reactive power, solving the system with the power flow method using the HCPQ bus and the droop bus, versus load 4 variation.

solutions of the complete hierarchically controlled microgrid system obtained with two widely accepted time-domain simulators, MATLAB/Simulink, and PSCAD. The obtained results reveal the advantages of the proposed method, such as proper performance regarding the CPU time and quadratic convergence rate, even in dominantly resistive or meshed systems. The solutions computed with the introduced power flow models match with the time-domain steady-state with errors in the worst cases of 5.112×10^{-6} and 1.581×10^{-3} comparing the proposed approach against Simulink and PSCAD, respectively. The computational time used by the proposed approach was barely 0.145 s.

As an essential advantage, the proposed power flow models do not need a slack bus since the secondary frequency control fixes the phase angle reference, avoiding the use of an adaptive slack bus or the fixing of a phase angle to zero. Furthermore, the second case study showed that the power flow solutions obtained with the hierarchical control (HCPQ bus) differ significantly from the solutions obtained using only the primary control (droop bus). The results obtained with the proposed HCPQ bus correspond to the obtained

in practical hierarchically controlled MGs. Therefore, the proposed power flow modeling is an useful and reliable tool for analyzes, planning, design, monitoring and control of microgrids.

REFERENCES

[1] S. Chowdhury and P. Crossley, *Microgrids and Active Distribution Networks*, ser. IET renewable energy series. Institution of Engineering and Technology, 2009.

[2] C. Li, S. K. Chaudhary, M. Savaghebi, J. C. Vasquez, and J. M. Guerrero, "Power flow analysis for low-voltage ac and dc microgrids considering droop control and virtual impedance," *IEEE Transactions on Smart Grid*, vol. 8, no. 6, pp. 2754–2764, Nov 2017.

[3] J. Schiffer, D. Zonetti, R. Ortega, A. Stankovic, T. Sezi, and J. Raisch, "A survey on modeling of microgrids - from fundamental physics to phasors and voltage sources," *ArXiv*, May 2015.

[4] K. Balamurugan and D. Srinivasan, "Review of power flow studies on distribution network with distributed generation," in *Power Electronics and Drive Systems (PEDS), 2011 IEEE Ninth International Conference on*, Dec 2011, pp. 411–417.

[5] X. Guo, Z. Lu, B. Wang, X. Sun, L. Wang, and J. Guerrero, "Dynamic phasors-based modeling and stability analysis of droop-controlled inverters for microgrid applications," *Smart Grid, IEEE Transactions on*, vol. 5, no. 6, pp. 2980–2987, Nov 2014.

[6] M. Rana, W. Xiang, and E. Wang, "Smart grid state estimation and stabilisation," *International Journal of Electrical Power and Energy Systems*, vol. 102, pp. 152 – 159, 2018.

[7] T. Aprille and T. Trick, "A computer algorithm to determine the steady-state response of nonlinear oscillators," *IEEE Transactions on Circuit Theory*, vol. 19, no. 4, pp. 354–360, 1972.

[8] G. Agundis-Tinajero, J. Segundo, R. Pena, C. Nunez, N. Visairo, J. Guerrero, and M. Savaghebi, "Harmonic issues assessment on pwm vsc-based controlled microgrids using newton methods," *IEEE Transactions on Smart Grid*, Early Access, 2016.

[9] A. Semlyen and A. Medina, "Computation of the periodic steady state in systems with nonlinear components using a hybrid time and frequency domain methodology," *IEEE Transactions on Power Systems*, vol. 10, no. 3, pp. 1498–1504, Aug 1995.

[10] A. Medina, J. Segundo, P. Ribeiro, W. Xu, K. Lian, G. Chang, V. Dinavahi, and N. Watson, "Harmonic analysis in frequency and time domain," *IEEE Transactions on Power Delivery*, vol. 28, no. 3, pp. 1813–1821, July 2013.

[11] J. Arrillaga, A. Medina, M. Lisboa, M. Cavia, and P. Sanchez, "The harmonic domain. a frame of reference for power system harmonic analysis," *IEEE Transactions on Power Systems*, vol. 10, no. 1, pp. 433–440, 1995.

[12] M. Esparza, J. Segundo, C. Nez, X. Wang, and F. Blaabjerg, "A comprehensive design approach of power electronic-based distributed generation units focused on power-quality improvement," *IEEE Transactions on Power Delivery*, vol. 32, no. 2, pp. 942–950, April 2017.

[13] J. J. Rico, M. Madrigal, and E. Acha, "Dynamic harmonic evolution using the extended harmonic domain," *IEEE Transactions on Power Delivery*, vol. 18, no. 2, pp. 587–594, 2003.

[14] N. Garcia and E. Acha, "On the efficient calculation of the periodic steady-state response of grid-connected wind parks part i," *IEEE Transactions on Sustainable Energy*, vol. 8, no. 2, pp. 458–467, April 2017.

[15] R. Peña, J. Núñez, and A. Medina, "Using a newton method and lapack libraries to initialize electromagnetic transient simulations in power systems," *Simulation Modelling Practice and Theory*, vol. 42, pp. 12 – 18, 2014.

[16] W. F. Tinney and C. E. Hart, "Power flow solution by newton's method," *IEEE Transactions on Power Apparatus and Systems*, vol. PAS-86, no. 11, pp. 1449–1460, Nov 1967.

[17] D. E. Olivares, A. Mehrizi-Sani, A. H. Etemadi, C. A. Caizares, R. Iravani, M. Kazerani, A. H. Hajimiragha, O. Gomis-Bellmunt, M. Saeedifard, R. Palma-Behnke, G. A. Jimnez-Estvez, and N. D. Hatziargyriou, "Trends in microgrid control," *IEEE Transactions on Smart Grid*, vol. 5, no. 4, pp. 1905–1919, July 2014.

[18] J. M. Guerrero, J. C. Vasquez, J. Matas, L. G. de Vicuna, and M. Castilla, "Hierarchical control of droop-controlled ac and dc microgrids: A general approach toward standardization," *IEEE Transactions on Industrial Electronics*, vol. 58, no. 1, pp. 158–172, Jan 2011.

[19] J. Rocabert, A. Luna, F. Blaabjerg, and P. Rodrguez, "Control of power converters in ac microgrids," *IEEE Transactions on Power Electronics*, vol. 27, no. 11, pp. 4734–4749, Nov 2012.

[20] A. M. Vural, "Interior point-based slack-bus free-power flow solution for balanced islanded microgrids," *International Transactions on Electrical Energy Systems*, vol. 26, no. 5, pp. 968–992, 2016.

[21] M. M. A. Abdelaziz, "Effect of detailed reactive power limit modeling on islanded microgrid power flow analysis," *IEEE Transactions on Power Systems*, vol. 31, no. 2, pp. 1665–1666, March 2016.

[22] M. M. A. Abdelaziz, H. E. Farag, E. F. El-Saadany, and Y. A. R. I. Mohamed, "A novel and generalized three-phase power flow algorithm for islanded microgrids using a newton trust region method," *IEEE Transactions on Power Systems*, vol. 28, no. 1, pp. 190–201, Feb 2013.

[23] I. Ziouani, D. Boukhetala, A.-M. Darcherif, B. Amghar, and I. E. Abbassi, "Hierarchical control for flexible microgrid based on three-phase voltage source inverters operated in parallel," *International Journal of Electrical Power and Energy Systems*, vol. 95, pp. 188 – 201, 2018.

[24] A. Hirsch, Y. Parag, and J. Guerrero, "Microgrids: A review of technologies, key drivers, and outstanding issues," *Renewable and Sustainable Energy Reviews*, vol. 90, pp. 402 – 411, 2018.

[25] A. Bidram and A. Davoudi, "Hierarchical structure of microgrids control system," *IEEE Transactions on Smart Grid*, vol. 3, no. 4, pp. 1963–1976, Dec 2012.

[26] A. Elrayyah, Y. Sozer, and M. E. Elbuluk, "A novel load-flow analysis for stable and optimized microgrid operation," *IEEE Transactions on Power Delivery*, vol. 29, no. 4, pp. 1709–1717, Aug 2014.

[27] F. Mumtaz, M. H. Syed, M. A. Hosani, and H. H. Zeineldin, "A novel approach to solve power flow for islanded microgrids using modified newton raphson with droop control of dg," *IEEE Transactions on Sustainable Energy*, vol. 7, no. 2, pp. 493–503, April 2016.

[28] M. E. Nassar, A. A. Hamad, M. M. A. Salama, and E. F. El-Saadany, "A novel load flow algorithm for islanded ac/dc hybrid microgrids," *IEEE Transactions on Smart Grid*, vol. PP, no. 99, pp. 1–1, 2017.

[29] M. E. Nassar and M. Salama, "A novel branch-based power flow algorithm for islanded ac microgrids," *Electric Power Systems Research*, vol. 146, no. Supplement C, pp. 51 – 62, 2017.

[30] M. H. Moradi, V. B. Foroutan, and M. Abedini, "Power flow analysis in islanded micro-grids via modeling different operational modes of dgs: A review and a new approach," *Renewable and Sustainable Energy Reviews*, vol. 69, no. Supplement C, pp. 248 – 262, 2017.

[31] M. A. Allam, A. Said, and M. Kazerani, "A generic modeling and power-flow analysis approach for isochronous and droop-controlled microgrids," *IEEE Transactions on Power Systems*, vol. PP, no. 99, pp. 1–1, 2018.

[32] G. C. Kryonidis, E. O. Kontis, A. I. Chrysochos, K. O. Oureilidis, C. S. Demoulias, and G. K. Papagiannis, "Power flow of islanded ac microgrids: Revisited," *IEEE Transactions on Smart Grid*, vol. PP, no. 99, pp. 1–1, 2018.

[33] L. Ren and P. Zhang, "Generalized microgrid power flow," *IEEE Transactions on Smart Grid*, vol. PP, no. 99, pp. 1–1, 2018.

[34] S. Golestan, J. M. Guerrero, and J. C. Vasquez, "Three-phase plls: A review of recent advances," *IEEE Transactions on Power Electronics*, vol. 32, no. 3, pp. 1894–1907, March 2017.

[35] J. M. Guerrero, L. G. de Vicuna, J. Matas, M. Castilla, and J. Miret, "A wireless controller to enhance dynamic performance of parallel inverters in distributed generation systems," *IEEE Transactions on Power Electronics*, vol. 19, no. 5, pp. 1205–1213, Sept 2004.

[36] Q. Shafiee, J. M. Guerrero, and J. C. Vasquez, "Distributed secondary control for islanded microgrids: A novel approach," *IEEE Transactions on Power Electronics*, vol. 29, no. 2, pp. 1018–1031, Feb 2014.

[37] Y. Levron, J. M. Guerrero, and Y. Beck, "Optimal power flow in microgrids with energy storage," *IEEE Transactions on Power Systems*, vol. 28, no. 3, pp. 3226–3234, Aug 2013.

[38] A. A. Eajal, M. A. Abdelwahed, E. F. El-Saadany, and K. Ponnambalam, "A unified approach to the power flow analysis of ac/dc hybrid microgrids," *IEEE Transactions on Sustainable Energy*, vol. 7, no. 3, pp. 1145–1158, July 2016.

[39] W. Stevenson and J. Grainger, *Power System Analysis*, ser. McGraw-Hill series in electrical and computer engineering: Power and energy.   McGraw-Hill Education (India) Pvt Limited, 2003.

[40] F. Katiraei and M. Iravani, "Power management strategies for a microgrid with multiple distributed generation units," *IEEE Transactions on Power Systems*, vol. 21, no. 4, pp. 1821–1831, Nov 2006.

[41] N. L. Díaz, E. A. Coelho, J. C. Vasquez, and J. M. Guerrero, "Stability analysis for isolated ac microgrids based on pv-active generators," in *2015 IEEE Energy Conversion Congress and Exposition (ECCE)*, Sept 2015, pp. 4214–4221.